A Comprehensive Survey of COVID-19 Detection Using Medical Images

Faisal Muhammad Shah[1], Sajib Kumar Saha Joy[2], Farzad Ahmed[3], Mayeesha Humaira[4], Amit Saha Ami[5], Shimul Paul[6], Md Abidur Rahman Khan Jim[7]

Department of Computer Science and Engineering

Ahsanullah University of Science and Technology

Dhaka, Bangladesh

[1]faisal.cse@aust.edu; [2]joyjft@gmail.com; [3]farzadahmed6@gmail.com;

[4]mayeeshahumaira@gmail.com; [5]amitsaha.aust@gmail.com; [6]shimulpaul59@gmail.com;

[7]jimrahman33@gmail.com

Abstract: The outbreak of the COVID-19 pandemic caused the death of a large number of people. Millions of people are infected by this virus and are still getting infected day by day. As the cost and required time of conventional RT-PCR tests to detect COVID-19, researchers are trying to use medical images like X-Ray and Computed Tomography (CT) images to detect it with the help of Artificial Intelligence (AI) based systems. In this paper, we reviewed some of these newly emerging AI-based models that can detect COVID-19 from medical images using X-Ray or CT of lung images. We collected information about available research resources and inspected a total of 80 papers from the time period of February 21, 2020 to June 20, 2020. We explored and analyzed datasets, preprocessing techniques, segmentation, feature extraction, classification and experimental results which can be helpful for finding future research directions in the domain of automatic diagnosis of Covid-19 disease using Artificial Intelligence (AI) based frameworks.

Keywords: COVID-19; Deep Learning; Medical Image

1 Introduction

Coronavirus Disease (COVID-19) is an infectious disease that started to proliferate from Wuhan China, in December 2019. Within a short period of time, this disease was detected worldwide and the World Health Organization (WHO) declared a pandemic on 11 March 2020. This disease is caused by severe acute respiratory syndrome coronavirus 2(SARS-CoV-2). In July, 2020 cases reached almost 12 million worldwide[1] and death due to this disease kept rising day by day. In July, 2020 the death toll is 562039. The total deaths and total cures by the month of the Worldometer[1] are illustrated in Fig. 1. This deadly virus can unfurl from individual to individual via cough, sneezing or even contact. As a result, it has become important to detect the affected people early and isolate them to stop further spreading of this virus.

Reverse Transcription-Polymerase Chain Reaction (RT-PCR) is a procedure of amassing samples from a region of a person's body where the coronavirus is most likely to congregate, such as a person's nose or throat. Then this sample is treated with chemicals to track down the existence of the coronavirus. Problems of RT-PCR are that it can detect coronavirus but it has a high false-negative rate which is the model predicts the result as

[1] https://www.worldometers.info/coronavirus/

negative but actually, it is positive (false-negative). Furthermore, in many parts of the world RT-PCR's availability is limited. Hence, Computer Tomography (CT) Images and X-Ray images can be the next best alternative to detect this virus. CT Images or X-Ray are readily available where there is no RT-PCR. Moreover, RT-PCR is expensive and consumes time. Additionally, proper training is required to collect samples for PCR. Whereas, it is relatively easy to handle CT Images and X-Ray.

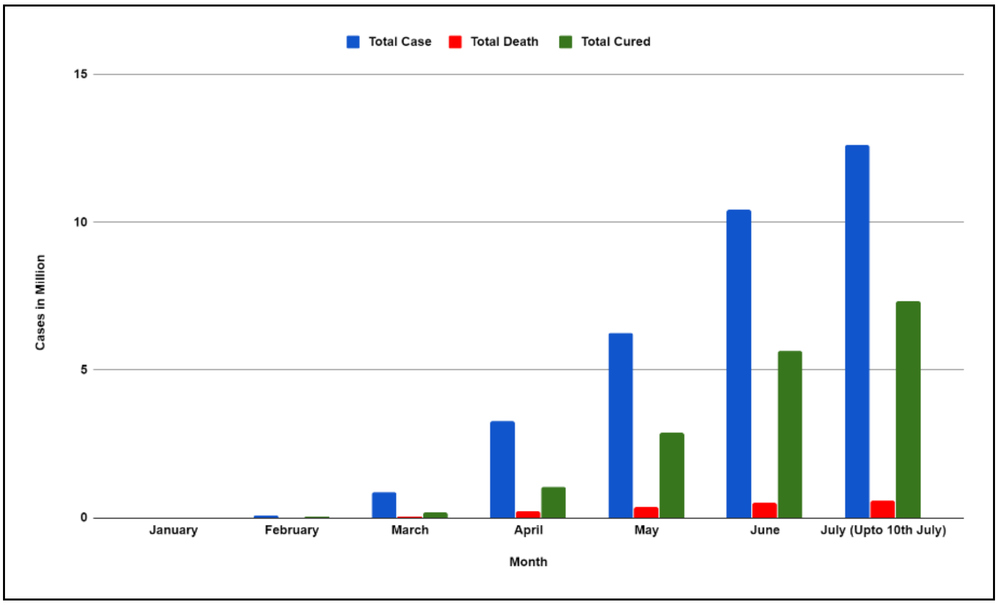

Fig. 1: Total Case, Total Death and Total Cured (By month) from Worldometer [1].

Machine Learning is an emerging field that could play a significant role in the detection of COVID-19 in the future. Till now researchers have used machine learning to detect COVID-19 using medical images such as X-Ray or CT images and obtained promising results. The average accuracy for detecting COVID-19 on CT is 90.69 % and on X-Ray 96.00 %. Many researchers also used transfer learning, attention mechanism [103] and Gradient-weighted Class Activation Mapping (Grad-CAM) [90] to make their results more accurate. Shi F et al. [91] and Ilyas M et al. [92] discussed some artificial intelligence-based models for diagnosis of COVID-19. Also, Ulhaq A et al. [93] reviewed some papers that worked on diagnosis, prevention, control, treatment and clinical management of COVID-19. However, as time goes by researchers are finding new and improved models for the diagnosis of COVID-19. We tried to review these new models alongside previous models.

Our survey will cover many research papers that are in pre-print format because of the fast-spreading and importance of COVID-19 disease. Although it is not the most favorable approach due to the likelihood of low standard and research without review, we intend to share all proposals in a single place while giving importance to the automatic diagnosis of COVID-19 in X-Ray and CT images of lungs.

The main aim of this paper is to systematically summarize the workflow of other research so that new researchers can analyze previous works and find a better solution. We oriented our paper as follows:

- Firstly, the Dataset source and different types of images used by papers are described in section 2.
- Secondly, in section 3 the methodology where data preprocessing and augmentation techniques, feature extraction methods, classification, segmentation and evaluation that researchers obtained are shown.
- Lastly, a discussion is made to aid the new researcher to find future works in detecting COVID-19

2 Dataset and resource description

The diagnosis of any disease is like the light at the end of the tunnel. In the case of the COVID-19 pandemic, the importance of diagnosis is beyond measure. The initial focus must be on data. This data will help Machine Learning (ML) algorithms to diagnose COVID-19 cases.

Due to the disadvantages of RT-PCR researchers adopted an alternative method which is the use of Artificial Intelligence on chest CT or X-Ray images to diagnose COVID-19. A chest CT image is an image taken using computed tomography (CT) scan procedure. In this procedure, X-Ray images are grasped from different angles and are compiled to form a single image. CT images of different people with and without COVID-19 is shown in Fig. 2.

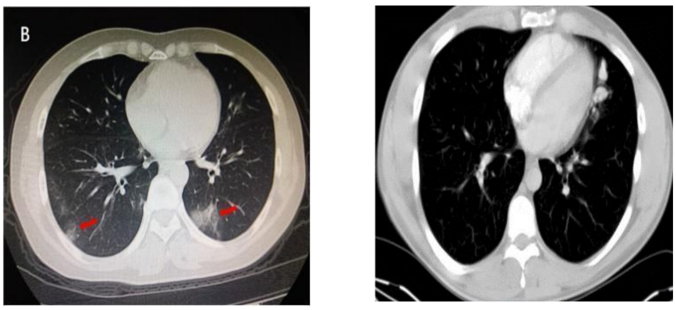

(a) (b)

Fig. 2: CT images[2] (a) COVID-19 (b) Normal.

[2] https://github.com/UCSD-AI4H/COVID CT/tree/master/Images-processed

Although a CT scan consumes less time it is fairly expensive. As a result, many researchers used X-Ray images instead of CT images. A chest X-Ray is a procedure of using X-Rays to generate images of the chest. It is relatively cheap and easily available in many parts of the world. X-Ray images of different people with COVID-19, viral pneumonia, bacterial pneumonia and a person without any disease (normal) are shown in Fig. 3.

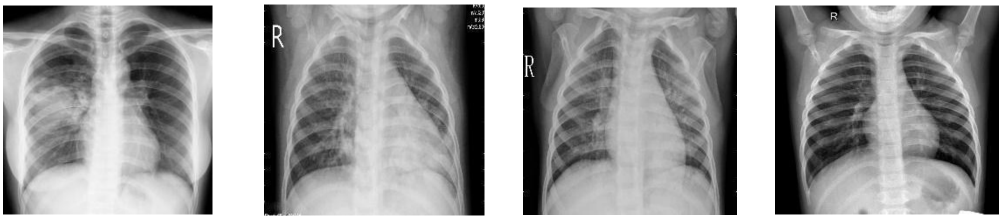

(a) (b) (c) (d)

Fig. 3: X-Ray images (a) COVID-19 (b) Viral Pneumonia (c) Bacterial Pneumonia (d) Normal from COVID19-XRay-Dataset[3].

Further in this section, an overview of the dataset sources used by papers is given. Datasets of both CT images and X-Ray images are illustrated here. Additionally, different types of images used in the dataset of both CT and X-Ray are discussed in this section.

2.1 Collection of datasets

Nowadays, the exchange of information between researchers and physicians is difficult due to the lockdown worldwide. Hence, massive COVID-19 data are out of reach for many researchers or difficult to find. As a result, to help researchers find better solutions to handle this pandemic we have gathered some of the useful datasets used by other researchers. A list of dataset sources used by papers from February, 2020 to June, 2020 embellished in Table 1.

Table 1: Summary of different data sources used by papers

TYPE	DATASET NAME	DATASET SOURCE	PAPERS
CT	The Lung Image Database Consortium (LIDC)	https://doi.org/10.1118/1.3528204	[7], [66]
CT	HUG	www.ChainZ.cn, El-Camino Hospital (CA), Zhejiang Province, China University Hospitals of Geneva (HUG)	[22]

[3] https://github.com/drkhan107/CoroNet/blob/master/dataset

CT	Societa Italiana di Radiologia Medica e Interventistica to generate datasets	https://www.sirm.org/	[23]
CT	Lung Segmentation and Candidate Points Generation	https://www.kaggle.com/arturscussel/lung-segmentation-and-candidate-points-generation	[26]
CT	COVID-19 CT segmentation dataset	http://medicalsegmentation.com/covid19/	[28], [42], [44], [62]
CT	COVID-CT	https://github.com/UCSD-AI4H/COVID-CT	[39]
X-Ray and CT	COVID-19 X rays	https://www.kaggle.com/andrewmvd/convid19-X-rays	[10], [14], [45], [63], [74]
X-Ray and CT	BIMCV COVID-19+	https://bimcv.cipf.es/bimcv-projects/bimcv-covid19/	[84]
X-Ray	Covid-chestxray-dataset	https://github.com/ieee8023/covid-chestxray-dataset	[8], [9], [10], [13], [14], [17], [18], [25], [26], [30], [33], [40], [45], [46], [50], [51], [52], [53], [55], [56], [63], [69], [70], [74], [76], [80], [81], [83]
X-Ray	Chest X-Ray Images (Pneumonia)	https://www.kaggle.com/paultimothymooney/chest-xray-pneumonia	[9], [10], [18], [25], [33], [46], [75], [81]
X-Ray	COVID-19 Radiography Database	https://www.kaggle.com/tawsifurrahman/covid19-radiography-database	[15], [19], [60], [76], [79]
X-Ray	British Society of Thoracic (BSTI)	https://www.bsti.org.uk/training-and-education	[18]
X-Ray	Radiopedia	https://radiopaedia.org/articles/normal-chest-imaging-examples?lang=gb	[18], [30], [50], [57], [80]
X-Ray	COVID-19 Chest X-ray Dataset Initiative	https://github.com/agchung/Figure1-COVID-chestxray-dataset	[19], [60]
X-Ray	ActualMed COVID-19 Chest X-ray Dataset Initiative	https://github.com/agchung/Actualmed-COVID-chestxray-dataset	[19], [60]
X-Ray	COVID-19 Image Data Collection	https://arxiv.org/abs/2003.11597	[20], [60]
X-Ray	COVID-19 database	https://www.sirm.org/category/senza-categoria/covid-19/	[20], [29], [30], [48], [50], [79]
X-Ray	Labeled Optical Coherence Tomography (OCT) and Chest X-Ray Images for Classification	https://data.mendeley.com/datasets/rscbjbr9sj/2.	[21], [74], [83]
X-Ray	COVID-19 X-ray dataset (COVID-CAPS)	https://github.com/ShahinSHH/COVID-CAPS	[36]
X-Ray	Kaggle RSNA Pneumonia Detection Dataset	https://www.kaggle.com/c/rsna-pneumonia-detection-challenge	[19], [40], [46], [52], [53], [60], [69], [80]
X-Ray	NIH Chest X-ray Dataset	https://www.kaggle.com/nih-chest-xrays/data	[50], [77]
X-Ray	Pneumonia Classification	https://drive.google.com/open?id=1J9I-pPtPfLRGHJ42or4pKO2QASHzLkkj	[57]
X-Ray	COVID-19	https://github.com/muhammedtalo/COVID-19	[77]
X-Ray	COVIDGR-1.0	https://github.com/ari-dasci/covidgr	[82]

2.1.1 CT image sources

CT images are more detailed than X-Ray images, so the diagnosis of COVID-19 becomes easy. For CT images-based works four papers used the COVID-19 CT segmentation dataset [28], [42], [44], [62] in their work. This dataset contains hundred axial CT images from forty patients. Chen X et al. [28] gained 89% accuracy and Qiu Y et al. [44] gained 83.62% accuracy using this dataset. Two papers used the Lung Image Database Consortium (LIDC) dataset [7], [66]. They both got their accuracy above 90 %. Besides these, some papers used Societa Italiana di Radiologia Medica e Interventistica to generate datasets [23], Lung Segmentation and Candidate Points Generation [26], COVID-CT [39] and HUG dataset [22] for their works. We have given all these dataset sources in Table 1 and the usage of these datasets monthly are exhibited in Fig. 4. The COVID-19 CT segmentation dataset [28], [42], [44], [62] was used mostly in April, 2020 and Lung Image Database Consortium (LIDC) dataset was used in March, 2020 and June 2020. Some researchers also used other lung disease images. Nevertheless, they collected CT images from different hospitals for the most part.

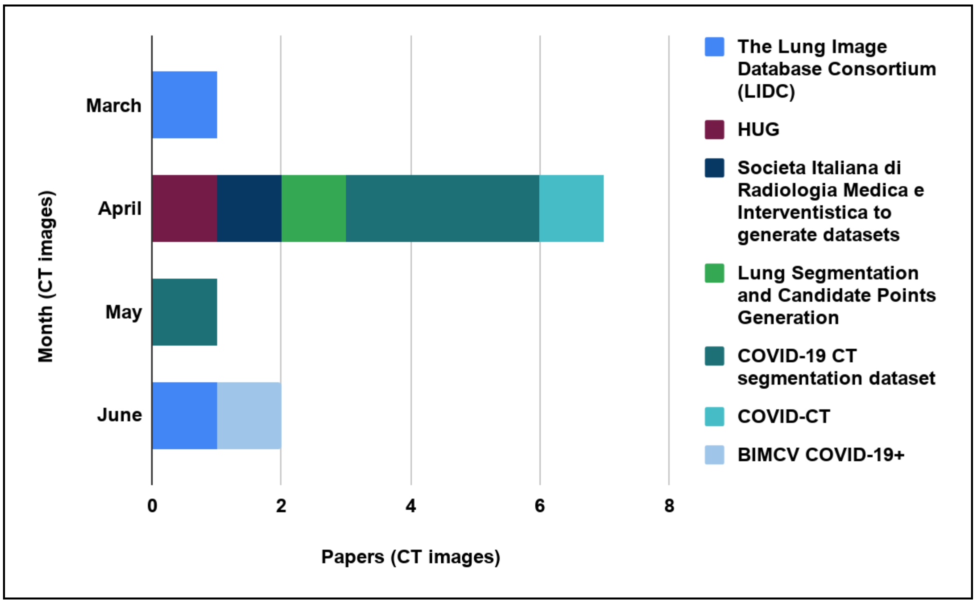

Fig.4: A bar chart showing seven publicly available CT datasets used from March, 2020 to June, 2020.

2.1.2 X-Ray image sources

X-Ray images dataset is more available than the CT images. Numerous datasets are used for the research to detect COVID-19. Most of the papers used Covid-chestxray-dataset [8], [25], [69], [83]. Some papers used Kaggle RSNA Pneumonia Detection Dataset [19], [40], [80], COVID-19 database [20], [30], [79], Chest X-Ray Images (Pneumonia) [9], [46], [81] to evaluate their model. These are the most common dataset for Chest X-Ray based COVID-19 research. All the sources are given in Table 1. Researchers who will work with COVID-19 in the future can get good help from our survey. Most of the researchers used different preprocessing techniques to increase the dataset size. For X-Ray based works Al-antari MA et al. [76] used COVID-19

Radiography Database for other lung diseases. Abbas A et al. [71] also worked with other lung diseases but they did not provide their dataset. The use of eighteen X-Ray datasets from March, 2020 to June, 2020 is illustrated in Fig. 5. From there it can be noticed that Covid-chestxray-dataset was used by most of the papers in all four months followed by Kaggle's Chest X-Ray Images (Pneumonia) which was used mostly in March, 2020, April, 2020 and June, 2020.

Some papers also used both CT and X-ray images from the COVID-19 X rays and BIMCV COVID-19+ datasets. From both Fig. 4 and Fig. 5 it can be observed that BIMCV COVID-19+ emerged in June, 2020.

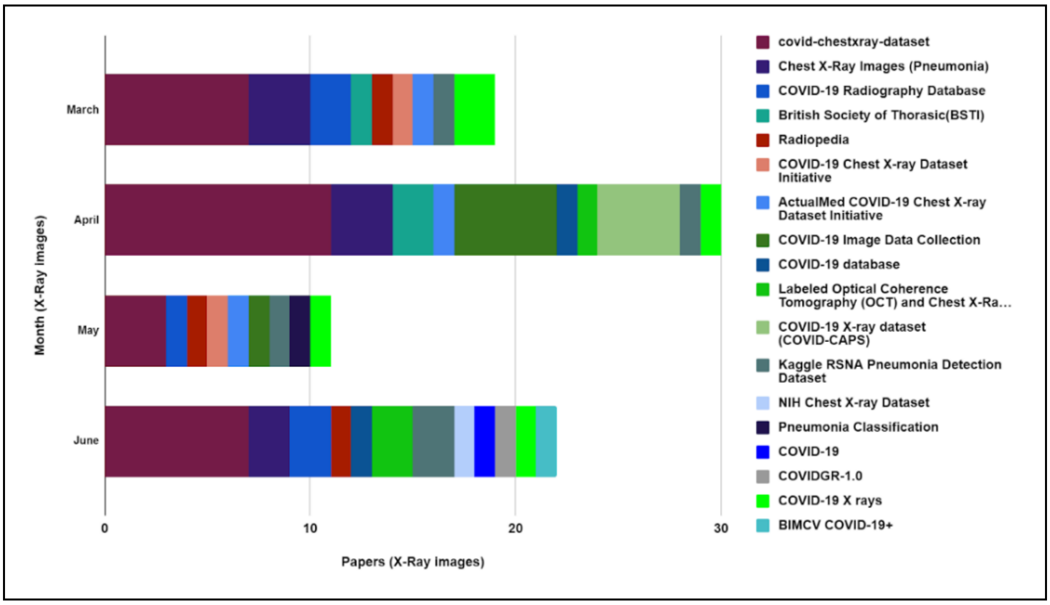

Fig. 5: A bar chart showing eighteen publicly available X-Ray datasets used from March, 2020 to June, 2020

2.2 Different types of images in the dataset

Diseases such as Pneumonia, Severe Acute Respiratory Syndrome (SARS), Middle East Respiratory Syndrome (MERS), Influenza and Tuberculosis affect the lungs like COVID-19 which can lead to misclassification of X-Ray and CT images. To avoid this problem researchers have adapted their dataset to have images of diseases affecting similar regions as COVID-19. Moreover, it is important to correctly distinguish COVID-19 patients from people who do not have COVID-19. As a result, papers also used normal images that are images of healthy people. The dataset in various papers contained a combination of COVID-19 images and images of healthy people or COVID-19 images, other lung disease images like Viral pneumonia [1], [10], [14], [15], [45] , Bacterial pneumonia [2], [14], [16], [35], [45], [78], fungal pneumonia [11], SARS [61], [64], [71], [77], MERS

[64], Influenza [66], Tuberculosis [16], [71], [72] and images of healthy people. The distribution of different types and the number of CT images used by papers are illustrated in Table 2. There 'Not specified' indicates that papers used that type of image but did not state the number explicitly and 'N/A' indicates those types of images were not used.

Table 2: Summary of different type of lung disease and normal (healthy patients) CT images used by papers

Paper	Normal Image	Pneumonia Image	COVID-19 Image	Other Lung diseases
[1]	175	224	219	N/A
[2]	86	100	88	N/A
[3]	N/A	14469	20886	N/A
[4]	1325	1735	1296	N/A
[5]	N/A	1027	1658	N/A
[6]	91	Not specified	877	450
[7]	100	N/A	106	N/A
[11]	N/A	40	1266	N/A
[12]	N/A	N/A	N/A	N/A
[16]	28873	30345	14944	15466
[18]	153	N/A	203	N/A
[22]	1126	N/A	938	N/A
[23]	6000	N/A	6000	N/A
[26]	247	N/A	178	N/A
[28]	Not specified	Not specified	Not specified	N/A
[32]	N/A	N/A	150	N/A
[34]	75541	N/A	64771	N/A
[37]	397	N/A	349	N/A
[38]	195	N/A	275	N/A
[39]	339	N/A	391	N/A
[42]	N/A	N/A	373	N/A
[43]	495	N/A	449	N/A
[44]	N/A	N/A	100	N/A
[47]	Not specified	740	325	N/A
[48]	344	N/A	439	N/A
[58]	N/A	1027	1495	N/A
[62]	N/A	N/A	N/A	N/A
[65]	397	N/A	349	83
[66]	3308	2296	2228	N/A
[68]	463	N/A	349	N/A
Total	**120438**	**50268**	**121700**	**15999**

The number of different types of CT images used in the dataset of papers is presented in Fig. 6. From there it can be seen that the number of COVID-19 CT images used is 121700. A total number of normal CT Images, Pneumonia CT Images and Other lung disease CT images are 120438, 50268 and 15999 respectively.

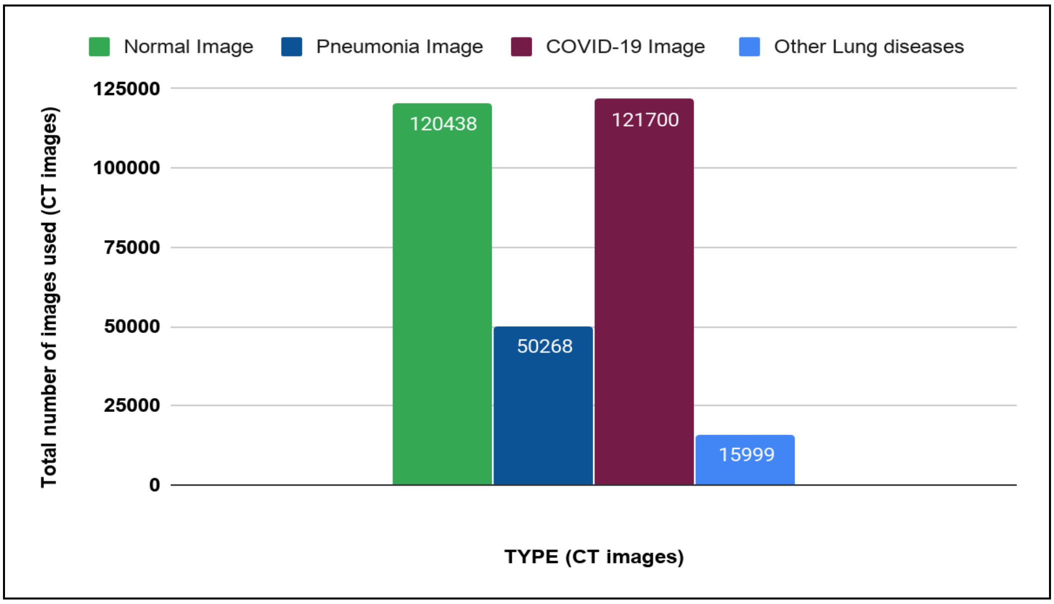

Fig. 6: The total number of CT images of different diseases and normal CT images used from February, 2020 to June, 2020.

The distribution of different types of X-Ray images used by papers is provided in Table 3. The total number of different images used by fifty papers from February to June is shown here. In Table 2, the distribution of different types of images was shown for thirty papers which were also from February, 2020 to June, 2020. Moreover, 'Not specified' and 'N/A' are used in Table 3 with the same purpose as it did in Table 2.

Table 3: Summary of different type of lung disease and normal (healthy patients) X-Ray images used by papers

Paper	Normal Image	Pneumonia Image	COVID-19 Image	Other Lung diseases
[8]	25	N/A	25	N/A
[9]	50	N/A	50	N/A
[10]	504	700	224	N/A
[13]	N/A	1431	100	N/A
[14]	1583	4290	68	N/A
[15]	1579	1485	423	N/A
[17]	15	N/A	25	N/A
[18]	85	N/A	85	N/A
[19]	N/A	5551	358	N/A
[20]	3450	N/A	455	N/A
[24]	8066	5538	259	N/A
[25]	207	N/A	207	N/A
[30]	N/A	320	135	N/A
[31]	179	179	179	N/A
[33]	310	654	284	N/A
[35]	7595	8792	313	N/A
[36]	N/A	N/A	120	N/A
[40]	8851	6054	180	N/A
[41]	2400	2600	536	N/A
[45]	127	127	127	N/A
[46]	137	N/A	137	N/A
[50]	350	322	225	50

[51]	8066	5521	183	N/A
[52]	44993	14777	167	N/A
[53]	9039	2306	318	N/A
[54]	8851	6045	215	N/A
[55]	1591	4706	105	N/A
[56]	191	131	180	N/A
[57]	1000	54	90	N/A
[59]	N/A	N/A	462	N/A
[60]	8066	5551	358	N/A
[61]	80	N/A	105	11
[63]	1000	1000	239	N/A
[64]	N/A	N/A	423	287
[67]	1579	2760	462	N/A
[69]	15000	15000	99	N/A
[70]	8851	6045	386	N/A
[71]	1126	Not specified	1050	112566
[72]	388	1000	500	303
[73]	2880	5179	415	N/A
[74]	1000	2000	309	N/A
[75]	25	N/A	25	N/A
[76]	N/A	120	326	866
[77]	3520	500	250	11
[78]	N/A	1583	305	N/A
[79]	13410	13450	8640	N/A
[80]	554	554	154	N/A
[81]	505	512	236	N/A
[82]	377	N/A	377	N/A
[83]	668	619	132	N/A
Total	**168223**	**127456**	**21062**	**114094**

The total number of COVID-19, normal, Pneumonia and other lung disease X-Ray images used by papers is shown in Fig. 7. There it can be seen that fifty papers used 21062 COVID-19 images, 168223 normal images, 127456 Pneumonia images and 114094 other lung disease images were used in total. It can be said that more CT images of COVID-19 were used than COVID-19 X-Ray images by comparing Fig. 6 and Fig. 7.

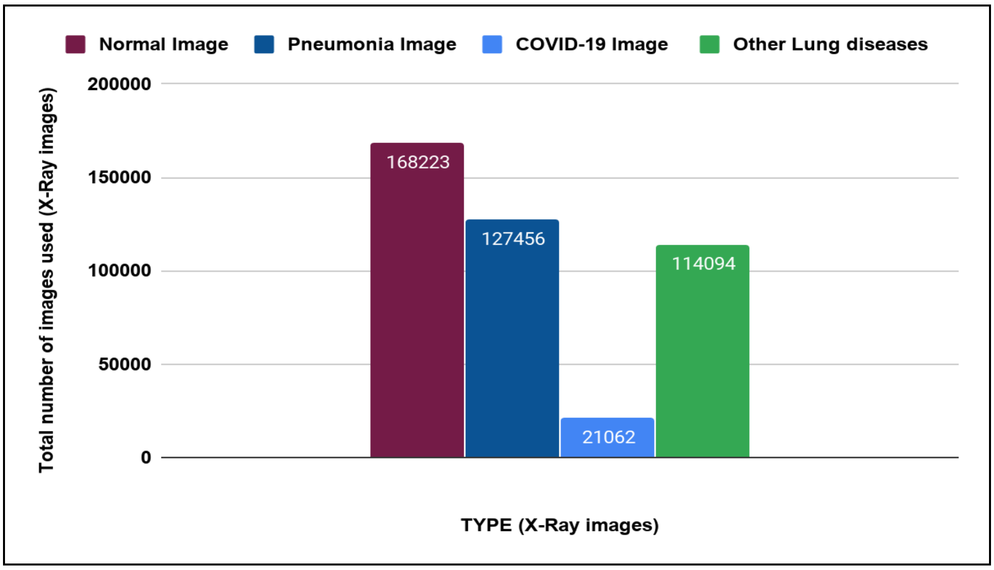

Fig. 7: The total number of X-Ray images for different disease and normal patients used from February, 2020 to June, 2020

3 Methodology

After data collection, several paramount steps must be followed to diagnose COVID-19 hence this section depicts different techniques employed by different papers. Firstly, preprocessing techniques, then the feature extraction methods were discussed. Secondly, segmentation methods and classification techniques are reviewed. Lastly, the results obtained by different papers are shown. The workflow of diagnosing COVID-19 from X-Ray images demonstrated in Fig. 8.

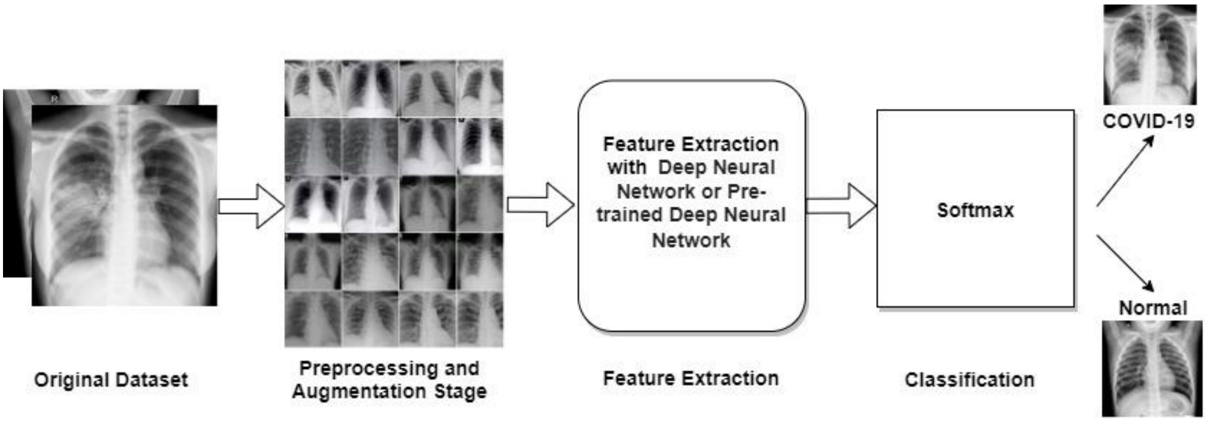

Fig. 8: The overall methodology of diagnosing COVID-19 from X-Ray images.

3.1 Preprocessing Techniques

One major problem of deep learning is overfitting. To minimize the effect of overfitting data augmentation is used in the pre-processing stage. Resizing, scaling, cropping, flipping, rotating are the most used data augmentation techniques. Some types of data augmentation techniques are discussed below:

Resizing is necessary because the images are not always within the same estimate which postures an issue whereas preparing the model. To generalize the dataset all the images are resized into a fixed dimension like 224 x 224 or 299 x 299.

Flipping or Rotating is done to increase the sample size of the datasets. Mainly horizontal and vertical flipping is used to do this as depicted in Fig. 9.

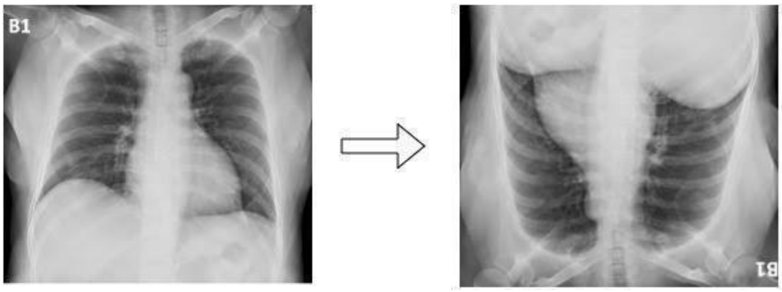

Fig. 9: An example of flipping by 180 degree.

Scaling or Cropping is the next most used augmentation technique is scaling or cropping. All the portions of the images are not necessary to use. So, to reduce the redundancy researchers used the cropping method as illustrated in Fig. 10.

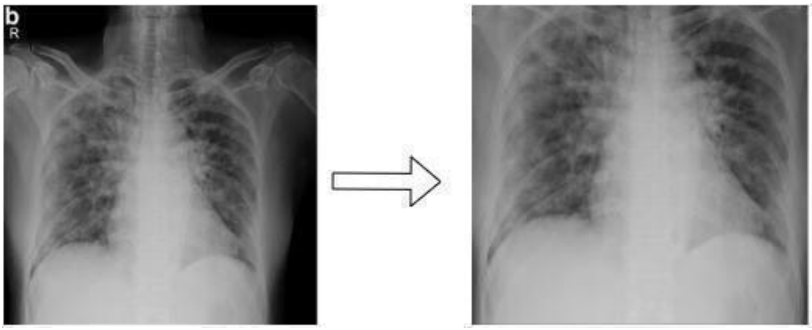

Fig. 10: An example of Cropping.

Brightness or Intensity adjusting is mandatory to increase or reduce the brightness of the images. An example is shown in Fig. 11.

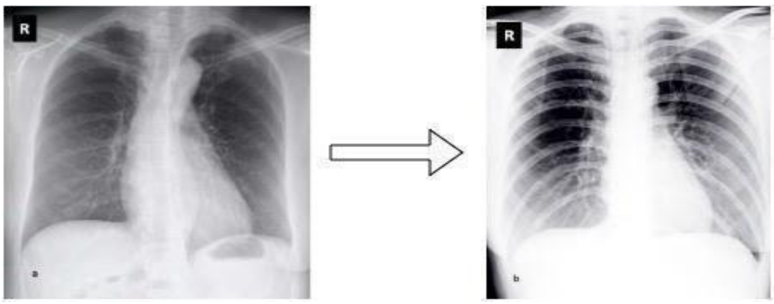

Fig. 11: An example of adjusting brightness.

General Adversarial Network (GAN) is the process of Generative modeling with deep learning methods. It is an unsupervised learning. It finds the patterns, similarities in the input datasets and generates new data which is similar to the input dataset. GAN [95] increases the sample size in the dataset but the quality of the samples is not guaranteed.

Table 4: Summary of the preprocessing and augmentation methods used by the papers

Augmentation Techniques	Paper	Count
Resize	[4], [8], [9], [10], [11] ,[13], [14], [15], [17], [18], [19], [20], [22], [23], [25], [28], [32], [33], [35], [39], [40], [42], [46], [56], [69], [70], [72], [73], [74], [75], [77], [78], [79], [81]	34
Flipping or Rotating	[1], [6], [7], [13], [14], [15], [19], [20], [23], [24], [25], [28], [30], [32], [34], [36], [40], [41], [44], [51], [54], [59], [60], [61], [65], [68], [69], [71], [75], [76], [77], [79], [83]	33
Scaling or Cropping	[1], [5], [6], [7], [10], [11], [13], [14], [18], [23], [25], [28], [32], [34], [35], [36], [39], [40], [44], [51], [54], [60], [68], [69], [73], [76], [81]	27
Contrast adjusting	[12], [14], [17], [20], [25], [31], [32], [38], [47], [59], [61], [64], [68], [72], [79]	15
Brightness or Intensity adjusting	[12], [19], [23], [25], [31], [51], [54], [60], [68]	9
GAN	[21], [39], [62], [82]	4

All the augmentation techniques are given along with the papers they were used in Table 4 and a pie chart in Fig. 12 shows the percentage usage of these augmentation techniques. From there it can be seen that resize and flipping has the highest percentage of 27.9% and 27.0% respectively. This pie chart is computed using values from Table 4. Scaling or Cropping, Contrast Adjusting, Brightness Adjusting, and GAN is 22.1%, 12.3%, 7.4% and 3.3% respectively. Besides these techniques, some papers used some different preprocessing techniques such as Histogram Equalization [64], Adaptive Winner Filter [38], Affine Transformation [13], [55], Histogram Enhancement [55], Color Jittering [13].

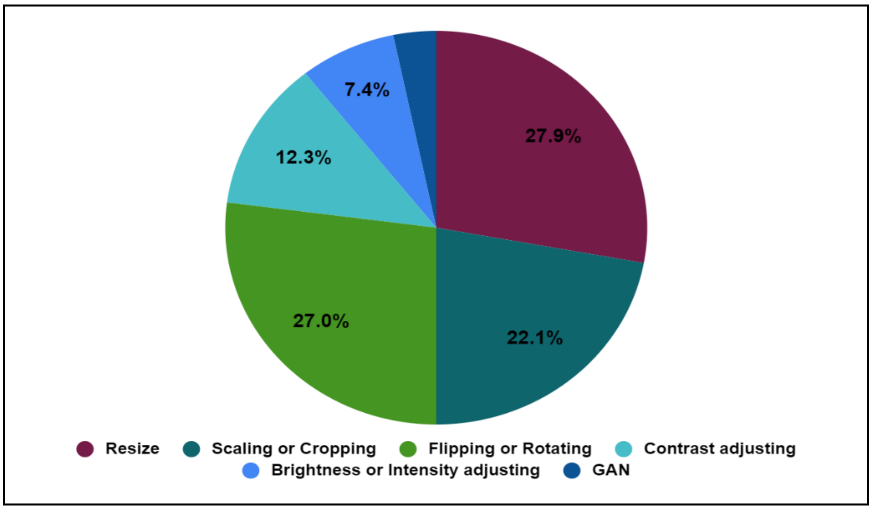

Fig. 12: Pie chart illustrates the augmentation techniques used by different papers. Here the percentage of usage of six different augmentation techniques is shown.

3.2 Segmentation

In digital image processing and computer vision, image segmentation is defined as the technique of partitioning a digital image into different segments where a segment means a set of pixels. The reason for using segmentation in image processing is simplification and changing the representation of an image into something more meaningful and easier to analyze. Like other areas of medical image processing, segmentation boosts the effectiveness of COVID-19 detection by finding the region of interest (ROI) like the lung area. Areas of the image that are out of the lung could meddle the model performance. By using segmentation methods, only ROI areas are preserved which reduces this effect. Segmentation can be carried out by radiologists, but it takes a long time. Several open-source automatic segmentation methods are available to use which are utilized by different authors.

The U-Net architecture is built with the help of convolutional neural network and it is modified such that it can achieve better segmentation in the domain of medical imaging [29]. The main advantage of U-Net is that the location information from the downsampling path and the contextual information in the up-sampling path are combined to get general information containing localization and context, which is the key to predicting a better segmentation map. U-Net based strategies were utilized in [3], [4], [6], [7], [12], [22], [28], [32], [38], [35], [42], [43], [66], [52], [55], [82] for quick and programmed lung segmentation to extract the lung region as the region of interest (ROI).

For CT images, to keep contextual information between slices some researchers [1] [6] applied 3D versions of U-Net for lung segmentation named 3D U-Net. Due to the low contrast at the infected areas in CT images and because of a large variety of both body shape and position over diverse patients, finding the infection areas from the chest CT scans was very challenging. Considering this issue, Fei Shan et al. [9] developed a deep learning-based network named VB-Net. It is a modified 3-D convolutional neural network based on V-Net [102]**.** This segmentation method is used in [5] [58].

Additional segmentation methods such as OpenCV, Dense-Net, NABLAN, DeepLab were also used for the segmentation of lung images in different papers. The different segmentation methods used by different papers are illustrated in Table 5 and the number of papers in which a specific segmentation method is used is shown by a bar chart in Fig. 13.

Table 5: Summary of different segmentation methods used in COVID-19 detection

Segmentation Methods	Papers	Count
U-Net	[3], [4], [6], [7], [12], [22], [28], [32], [38], [35], [42], [43], [66], [52], [55], [82]	16
3D U-Net	[1], [6]	2
VB-Net	[5], [58]	2
OpenCV	[2]	1
DeepLab	[28]	1
NABLAN	[26]	1
Dense-Net	[11], [56]	2
MiniSeg	[44]	1

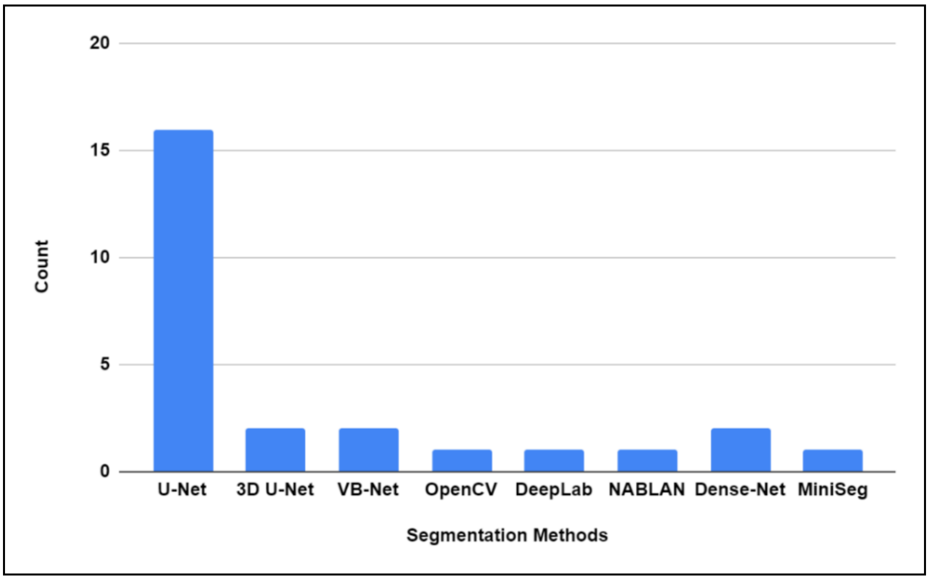

Fig. 13: A bar chart showing number of times different segmentation models used in different papers

3.3 Feature Extraction Methods

Feature extraction is an essential step for classification as the extracted features provide useful characteristics of the images. For image feature extraction Deep Neural Networks (DNN) have extraordinary capabilities. As a result, these are used extensively in Computer Vision Algorithms and Convolutional Neural Network (CNN) which is also known as ConvNet is a part of DNN.

3.3.1 Convolutional Neural Network (CNN)

CNN is most repeatedly used to explore visual imagery [96]. There are some layers in a CNN architecture. We have described these below.

Convolution layer is the core building block of a CNN. The layer's parameters are made up of a set of discoverable kernels or filters which have a little responsive field but enlarge through the full input volume.

Nonlinear layer is the layer where the change of the output is not proportional to the change of the input. This layer uses activation functions to convey non-linearity to data by adding after each convolution layer. Used activation functions can be Rectified Linear Unit (ReLu) [104], Tanh, etc.

Pooling layer is another important portion of CNN architecture. This layer is used to downsize the matrix. Pooling can be done in several methods: Max Pooling, Min Pooling, Average Pooling, and Mean Pooling.

Fully connected layer is the layer where every Neuron of a layer is connected with every other neuron of another layer. Traditional Multilayer Perceptron neural networks (MLP) and this layer have common principles.

3.3.2 Existing Pre-trained CNN Models

Most of the COVID-19 diagnosis architectures used different pre-trained CNN models. These are shown in Table 6 (CT images) and Table 7 (X-Ray images). Researches used mostly Residual Network (ResNet), Densely Connected Convolutional Network (DenseNet), Visual Geometry Group (VGG), SqueezeNet architecture for CT that is shown in Table 6 and ResNet, DenseNet, VGG, Inception, InceptionResNet in Table 7 for X-Ray images**.** Some of the most used existing pre-trained CNN models are described here:

Residual Network (ResNet) is a Convolutional Neural Network (CNN) architecture that was designed to enable hundreds or thousands of convolutional layers. While previous CNN architectures had a drop off in the effectiveness of additional layers, ResNet [27] can add a large number of layers with a strong performance. ResNet is convenient and efficient for data-driven.it has different variants (ResNet18, ResNet169, ResNet50, ResNet152 etc.) and this network has an image input size of 224 X 224. ResNet is the most used architecture in our survey for both CT and X-Ray based research. Fourteen papers that have used ResNet in their proposed models for CT image-based works are shown in Table 6 and twenty-seven papers in Table 7 were used for X-Ray based works.

Densely Connected Convolutional Networks (DenseNet) is one of the latest neural networks for visual object recognition [49]. It is quite related to ResNet but has some fundamental differences. With a very simple architecture to ensure maximum information flow between layers in the network. By matching feature map size all over the network, they connected all the layers directly to all of their subsequent layers - a Densely Connected Neural Network, or simply known as DenseNet. DenseNet made strides in the data stream between layers by proposing these distinctive network designs. Unlike many other networks like ResNet, DenseNets do not sum the output feature maps of the layer with the incoming feature maps but concatenate them. This architecture has different types of variants (DenseNet101, DenseNet169, DenseNet201, etc.) and it has an input shape of 224 x 224. In Table 6 DenseNet architecture is used by four papers and from Table 7, it is used by seventeen papers.

Visual Geometric Group (VGG) is another important CNN architecture to the researchers. VGG [85] Network consists of 16 or 19 convolutional layers and is very appealing because of its very uniform architecture. It has an input image shape of 224 x 224. In our survey, we collected four papers who work with VGG for COVID-19 detection purposes to get the features from CT images that were illustrated in Table 6 and fifteen papers from X-Ray based works were shown in Table 7.

Inception is a transfer learning-based method that is very popular to the researchers [86] [87]. It consists of two parts: feature extraction from images with the help of CNN and classification with softmax and fully connected layers. There are many versions of inception. Among them InceptionV1, InceptionV2, InceptionV3, and InceptionV4 are popular. The input image shape is 299 x 299 in this architecture. Twelve papers used an

Inception based model for X-Ray based classification of COVID-19 given in Table 6 and only one paper [47] for CT images used this.

InceptionResnet is the same as InceptionV4 [88]. InceptionResNetv1 a half breed Initiation adaptation that encompasses a similar computational fetched to Inceptionv3. InceptionResNetV2 may be a convolutional neural arrangement that is prepared on more than a million pictures from the ImageNet [89] database. The arrangement is 164 layers profound and can classify pictures into 1000 protest categories. A few cases of the objects are pencil, creatures, etc. For this, the organization has learned an endless extent to include representations for a wide run of pictures. The organizer has a picture input measure of 299 x 299. Eight papers given in Table 7 utilized this strategy for X-Ray pictures including extraction.

Table 6: Summary of image feature extraction methods used by different papers for CT images

CNN	Paper	Count
ResNet	[1],[2],[4],[6],[7],[16],[22],[23],[34],[37],[62],[65],[66],[68]	14
DenseNet	[2],[11],[37],[68]	4
VGG	[2],[23],[34],[37]	4
SqueezeNet	[48],[65]	2
AlexNet	[18]	1
CrNet	[37]	1
EfficientNet	[37]	1
FCN-8s	[6]	1
GoogLeNet	[23]	1
Inception	[47]	1

The number of different CNN models used per month for CT Images is shown in Fig. 14. For feature extraction from CT images, researchers use various types of CNN models. ResNet is the most used architecture within these five months. In February, 2020 three types of CNN models were used, two papers used ResNet and one paper used DenseNet and another paper used VGG. During March, 2020 four papers used ResNet, and AlexNet and FCN-8s used once. Whereas in April, 2020 ResNet was used four times, three papers used VGG and SqueezeNet, CrNet, EfficientNet, GoogLeNet, and Inception was used once. Moreover, in May, 2020 ResNet was used twice and SqueezeNet was used once and finally in June, 2020 DenseNet and ResNet were used by one and two papers respectively.

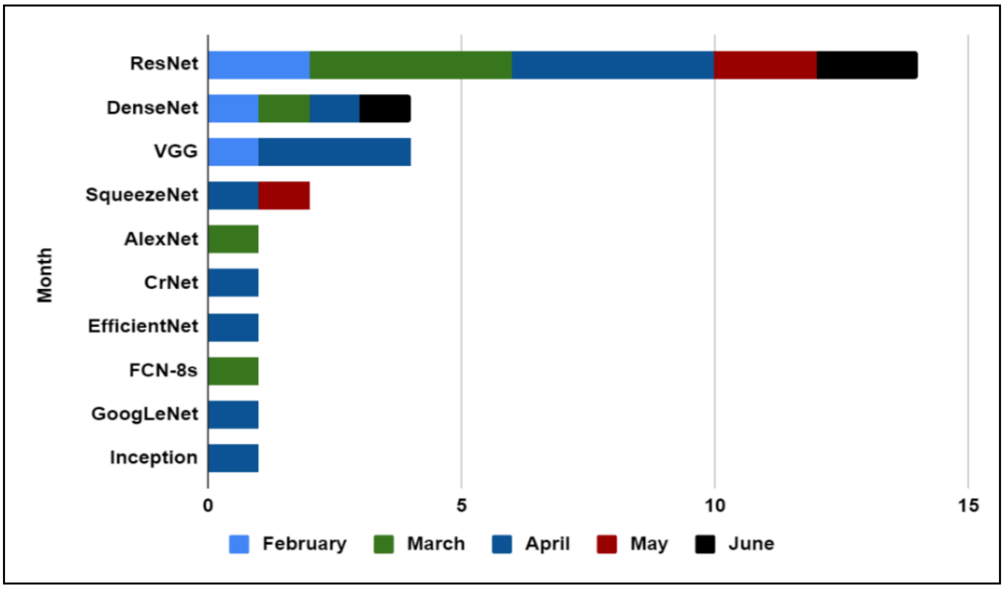

Fig. 14: A bar chart for describing used CNN for CT images (By month).

Table 7: Summary of image feature extraction methods used by different papers for X-Ray images

CNN	Papers	Count
ResNet	[8],[9],[13],[14],[15],[19],[21],[24],[30],[40],[41],[45],[46],[51],[53],[54],[55],[56],[61],[63],[64],[67],[69],[70],[71],[72],[81],[82]	27
DenseNet	[8],[15],[24],[25],[31],[35],[45],[46],[52],[54],[55],[64],[67],[69],[72],[74],[81]	17
VGG	[8],[10],[15],[24],[30],[35],[45],[46],[51],[63],[71],[72],[73],[75],[77]	15
Inception	[8],[9],[10],[15],[35],[45],[46],[56],[64],[67],[79],[81]	12
InceptionResNet	[8],[9],[10],[35],[45],[46],[69],[81]	8
Xception	[8],[10],[33],[35],[40],[45],[46],[83]	8
AlexNet	[18],[21],[45],[71],[72],[80]	6
SqueezeNet	[15],[21],[31],[41],[64]	5
GoogLeNet	[21],[45],[63],[71]	4
NASnet	[46],[69],[74]	3
ShuffleNet	[31],[45]	2
EfficientNet	[51]	1
Simple CNN	[18]	1

Different CNN models and the number of times of its usage per month is shown for X-Ray images in Fig. 15. This figure depicts that ResNet is one of the most used models. Also, for feature extraction of X-Ray Images, most of the researchers used ResNet. In our survey during March, 2020 ResNet was used six times, DenseNet two times, VGG three times, Inception four times, InceptionResNet three times, Xception two times and AlexNet, SqueezeNet one times each. In April, 2020 ResNet was used ten times, DenseNet eight times, VGG six times, Inception three times, InceptionResNet three times and Xception five times. AlexNet, GoogLeNet and ShuffleNet were both used twice. SqueezeNet, Inception and InceptionResNet were used three times each. NASnet and EfficientNet were used once each time. During May, 2020 ResNet was used five times, DenseNet and Inception were used two times each, VGG, SqueezeNet and GoogLeNet three of them were used only once. Finally, in June, 2020 ResNet was used seven times, DenseNet and VGG both were used five times each.

Inception, InceptionResNet, Xception, AlexNet, GoogLeNet, and NASnet were used three, two, one, three, one and two times respectively.

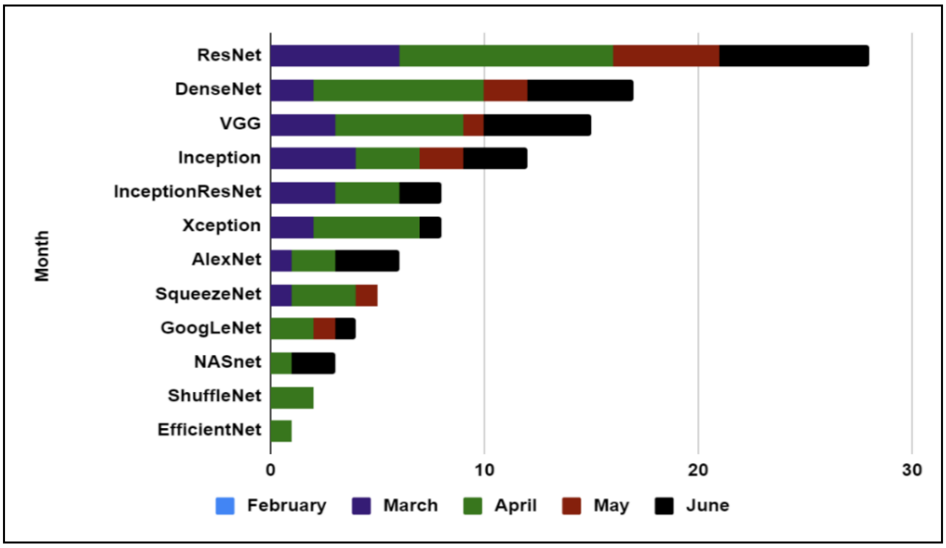

Fig. 15: A bar chart describing the use of different CNN models for X-Ray images (By month).

3.3.3 Specialized CNN Methods for COVID-19

Some researchers developed several architectures especially for COVID-19 detection with the backbone of basic CNN. These architectures have extra capabilities to classify images into multiple classes like COVID-19, Viral pneumonia, Bacterial Pneumonia and Normal case. Because in the primary stage these models are trained on ImageNet and then it is trained on various lung diseases CT or X-Ray images. Here are few models which are made based on the basic CNN models:

COVID-19 Detection Neural Network (COVNet) architecture was introduced by [4]. This is a 3D deep learning architecture to detect COVID-19. This architecture can extract both 2D local and 3D global illustrative features. The COVNet architecture is made with a ResNet architecture as the base model. A max-pooling operation was used for the extracted features from all slices. The finishing feature map is connected with a fully connected layer and they used a softmax activation function for the probability score for every type (COVID-19, Community-Acquired Pneumonia (CAP), and non-pneumonia).

COVID-Net architecture is specially adapted for COVID-19 case detection from chest X-Ray images. So obviously it has high architectural diversity and selective long-range connectivity. The massive use of a projection-expansion-projection design pattern in the COVID-Net [60] architecture is also observed. COVID-Net network architecture is incorporated into a heterogeneous mix of convolution layers. The proposed COVID-Net was pre-trained on the ImageNet dataset and then applied to the COVIDx dataset. Applying this architecture, they got accuracy about 93.3% on the COVIDx dataset.

ChexNet is originally a DenseNet-121 type of deep network which is trained on Chest X-ray images introduced by the paper [67]. So, this architecture has been specially designed to diagnose COVID-19.1024-D feature vectors are extracted for the compact classifiers in ChexNet. They used the Softmax activation function to classify COVID-19, Normal, Viral Pneumonia and Bacterial Pneumonia. The number of trainable parameters in this model is 6,955,906.

COVID-CAPS is a capsule-based network architecture invented by [36]. This model has 4 convolutional layers and 3 capsule layers. 3-dimensional chest X-Ray images are the input of this architecture. The primary layer is a convolutional layer, then batch-normalization is attached. The second layer is also a convolutional layer, followed by a pooling layer. Correspondingly, the third and fourth layers are convolutional, and the fourth layer is reshaped as the first Capsule layer. Three Capsule layers are embedded in the COVID-CAPS to perform the routing. The last Capsule layer contains the classification parameters of the two classes of positive and negative COVID-19. The trainable parameter is 295,488 for this model. Pre-trained COVID-CAPS gave 98.3% accuracy.

Detail-Oriented Capsule Networks (DECAPS) architecture was introduced by the paper [39]. It uses a ResNet with three residual blocks because the base network which outputs 1024 feature maps, followed by a 1×1 convolutional layer with 512 channels and a ReLU non-linear layer. This architecture is trained in CT images. This model obtained an area under the curve (AUC) of 98%.

Besides these, some papers used different types of approaches Like Details Relation Extraction neural network (DRE-Net) [2] which is ResNet-50 on Feature Pyramid Network [FPN] for extracting top K details from each image and an attention module combined to learn the importance of every detail. In the training stage,[5] and [66] employed the least absolute shrinkage and selection operator (LASSO) to traverse the optimal subset of clinical-radiological features to classify. GLCM, HOG and LBP were used by [45]. Moreover, [7] used commercial off-the-shelf software that detects nodules and small opacities within a 3D lung volume and subsystem.

Some papers used Multilevel Thresholding [17]. Some of them used COVID-ResNet [19], CoroNet [33], CovXNet [78]. One of the papers in our survey used location-based attention [1]. Again, some of the paper applied Deep Feature Fusion [23] for extraction. Paper [25] applied Gravitational Search Algorithm (GSA) along with a pre-trained feature extraction architecture like DenseNet. Also, some papers for example [38] used the FFT-Gabor scheme in their research.

Besides some paper applied transfer learning [24], [35], [40], [41] approach with the basic CNN models for better results. Basically, transfer learning is a technique for foretelling modeling on a different but somehow same problem that can then be reused partially or fully to expedite the training and develop the performance of a model on the problem. In deep learning, transfer learning means regenerating the weights in one or more layers from a pre-trained network architecture in a new model and either keeping the weights fixed, fine-tuning them, or adapting the weights entirely when training the model.

3.4 Interpretability

A machine learning model consists of algorithms that tries to learn patterns and relationships from the data source. To make the results obtained from machines interpretable, researchers use different techniques such as Class Activation Mapping (CAM), Gradient-weighted Class Activation Mapping (Grad-CAM) with heatmap. CAM is a method that creates heatmaps to show the important portions from the images, especially which parts are essential in terms of the Neural Network. CAM has various versions such as Score CAM and Grad-CAM. The heatmap generated by CAM is a visualization that can be interpreted as where in the image the neural net is searching to make its decision. This is very important in image classification and object localization problems.

In our survey, there are few papers that utilized CAM [94] and few papers [4], [7], [14], [22], [24], [35], [48], [50], [52], [53], [55], [56], [69], [78], [83] utilized Grad-CAM with heatmap for better understanding of the region it is centering on. At the same time, heatmaps can also provide radiologists with more useful information and further help them.

3.5 Classification

Almost all of the COVID-19 diagnosis models use Convolutional Neural Network [96] as a feature extractor and as a classifier, it uses softmax or sigmoid. Some authors also attempted to amplify CNN with sigmoid layer. The authors of [45] merged CNN with softmax layer along with SVM classifier [97], SH et al. [46] used CNN with softmax layer along a decision tree, random forest, XGBoost [98], AdaBoost [99], Bagging Classifier [100] and LightGBM [101]. The authors of [67] also merged CNN with KNN, support estimator network and SVM classifier. Nonetheless, these models need a large amount of data for training which is in shortage of COVID-19 images.

Mainly there are two ways of classifying Covid-19 images, Binary Classification and Multiclass classification. In Binary Classification authors try to separate COVID-19 and non-COVID-19 patients, but this technique is very inaccurate as other types of lung diseases (viral pneumonia, viral pneumonia, bacterial pneumonia and Community-Acquired Pneumonia) can be classified as COVID-19. For that reason, many authors differentiate COVID-19, viral pneumonia, bacterial pneumonia, Community-Acquired Pneumonia and normal images by classifying them using a softmax classifier, using the method of Multiclass Classification. In terms of accuracy of detecting COVID-19 images, multiclass classifiers performed better than binary classifiers. A summary of different classification techniques used by different papers is illustrated in Table 8 and Table 9.

Some authors also tried to detect Covid-19 in several stages. In the beginning, they separate normal and pneumonia images. After that, they classify Covid-19 by filtered pneumonia images. Several-stage classification helps the models to memorize various leveled connections. In paper [52] and [55], authors used several-stage classification rather than an end to end method to detect COVID-19 which outperforms several end to end techniques. On the flip side, the performance of multiclass classification relies on datasets. If there is a shortage of dataset, the model cannot become familiar with the various leveled connections between classifications like Pneumonia to Viral Pneumonia to COVID-19.

Table 8: Summary of classification methods used by different papers both for CT and X-Ray images

Classification Methods	Papers	Count
Binary Classification	[5], [7], [9], [10], [11], [12], [15], [18], [21], [23], [25], [26], [30], [31], [32], [33], [34], [36], [37], [39], [41], [43], [45], [46], [47], [48], [52], [56], [58], [59], [65], [67], [68], [69], [71], [72], [73], [74], [75], [76], [81], [82], [83]	43
Multiclass Classification	[1], [2], [3], [4], [6], [8], [10], [13], [14], [15], [16], [19], [20], [22], [24], [26], [28], [35], [37], [40], [43], [50], [51], [53], [54], [55], [57], [60], [61], [63], [64], [65], [66], [69], [77], [79], [80]	37

Table 9: Summary of classification methods used by different papers both for CT and X-Ray month-wise

Classification Methods (Month Wise)	Binary Classification	Count	Multiclass Classification	Count
February, 2020		0	[1], [2]	2
March, 2020	[5], [7], [9], [10], [11], [12], [15], [18]	8	[3], [4], [6], [8], [10], [13], [14], [15], [16], [19]	10
April, 2020	[21], [23], [25], [26], [30], [31], [32], [33], [34], [36], [37], [39], [41], [43], [45], [46], [47], [52]	19	[20], [22], [24], [26], [28], [35], [37], [40], [43] [50], [51], [53], [54]	13
May, 2020	[56], [58], [59], [65]	4	[55], [57], [60], [61], [63], [64], [65]	7
June, 2020	[67], [68], [69], [71], [72], [73], [74], [75], [76], [81], [82], [83]	12	[66], [69], [77], [79], [80]	5

3.6 Experimental results of the papers

Researchers used different metrics to analyze their COVID-19 model's performance. Among them, the most popular and most used metrics for classification type problems were Accuracy, Precision, Recall/Sensitivity, F1 Score, Specificity, and Area Under Curve (AUC). In our work, we tried to record the performance with these metrics from all the papers given in Table 10 for CT and in Table 11 for X-Ray images**.** Also, we have shown the number of COVID-19 images from the total images used for training, testing and validation. Some papers explicitly stated the train-test split of COVID-19 images and for some papers, we calculated the split according to the ratio that was provided. Even so, for some papers, it was not clearly stated how they distributed their dataset [5], [26], [28], [45], [62]. Additionally, some papers explicitly stated the use of data for validation [2], [4], [8], [9], [11], [15], [16], [25], [30], [31], [43], [47], [48], [52], [54], [55], [56], [64], [65], [76], [79].

A summary of the results obtained by models using CT images is illustrated in Table 10. There papers with their Accuracy, AUC, Sensitivity and Specificity are given along with their distribution of COVID-19 images in testing training and validation set. It can also be seen that CT image-based models gained a minimum accuracy of 79.50% for the paper [68] and maximum accuracy of 99.56% for the paper [26].

Table 10: Summary of result evaluation for CT images

COVID-19							
Publication Date	**Paper**	**Total Image**	**Training**	**Testing**	**Validation**	**Result (%)**	**Cited By(No of papers)**
February 21, 2020	[1]	618	189	30	N/A	Accuracy:86.70	117
February 25, 2020	[2]	274	79	25	9	Accuracy:94.00 AUC:91.00	22
March 01, 2020	[3]	46096	691	636	N/A	Accuracy:98.85 Sensitivity:94.34 Specificity:99.16	37
March 19, 2020	[4]	4356	1048	131	117	Sensitivity:90.00 Specificity:96.16 AUC:96.00	172
March 22, 2020	[5]	2685	Not specified	Not specified	Not specified	Accuracy:87.90 Sensitivity:90.70 Specificity:83.30 AUC:94.20	24
March 23, 2020	[6]	1418	723	154	N/A	Sensitivity:97.4 Specificity:92.2 AUC:99.10	13
March 24, 2020	[7]	206	50	56	N/A	Sensitivity:98.20 Specificity:92.20 AUC:99.60	87
March 26, 2020	[11]	5372	1266	102	92	Accuracy:85.00 Sensitivity:79.35 Specificity:71.43 AUC:86.00	8
March 26, 2020	[12]	630	289	76	N/A	Accuracy:90.10 Sensitivity:90.70 Specificity:91.10	35
March 30, 2020	[16]	89628	7543	4887	2514	Accuracy:98.80 Sensitivity: 98.20 Specificity: 98.90	2
March 31, 2020	[18]	361	339	17	N/A	Accuracy:94.10 Sensitivity:90.00 Specificity:100.00	11
April 06, 2020	[22]	2064	829	109	N/A	Sensitivity:94.00 Specificity:98.00 AUC:99.40	11
April 07, 2020	[23]	12000	4500	1500	N/A	Accuracy:98.93 Sensitivity:97.60 Specificity:97.63	5
April 10, 2020	[26]	420	375	45	N/A	Accuracy:99.56	2
April 12, 2020	[28]	110	Not specified	Not specified	10-Fold cross validation	Accuracy:89.00	7
April 14, 2020	[32]	360	120	30	N/A	Accuracy:89.20 Sensitivity:88.60 Specificity:87.60 AUC:92.30	4
April 15, 2020	[34]	79396	2794	64711	N/A	Sensitivity:95.00 Specificity: 93.00	11
April 17, 2020	[37]	746	191	98	60	Accuracy:83.00 AUC:87.00	4
April 17, 2020	[38]	470	165	110	N/A	Accuracy:93.65 Sensitivity:94.25 Specificity:92.79	1
April 17, 2020	[39]	746	286	105	N/A	Accuracy:87.60	2

						Specificity:85.20 AUC:96.10	
April 21, 2020	[42]	829	298	75	Not specified	Sensitivity:86.70 Specificity:99.30	1
April 21, 2020	[43]	1044	349	50	50	Accuracy:86.00 Sensitivity:94.00 Specificity:94.00 AUC:93.00	3
April 21, 2020	[44]	100	60	40	N/A	Accuracy:83.62 Sensitivity:97.42	3
April 24, 2020	[47]	1065	340	N/A	290	Accuracy:89.50 Sensitivity: 87.00 Specificity:88.00	77
April 24, 2020	[48]	783	251	108	80	Accuracy:83.00 Sensitivity:85.00 Specificity:81.73	2
May 07, 2020	[58]	2522	1196	299	5 fold cross validation	Accuracy:97.79 Sensitivity:93.05 Specificity:89.95 AUC:96.35	1
May 21, 2020	[62]	130	Not specified	Not specified	Not specified	Sensitivity:72.50 Specificity:96.00	10
May 28, 2020	[65]	746	178	95	76	Accuracy:99.40 Sensitivity:100.00 Specificity:98.60 AUC:99.65	0
June 02, 2020	[66]	4260	751	Not specified	Not specified	Sensitivity:90.19 Specificity:95.76 AUC:97.17	12
June 17, 2020	[68]	812	349	N/A	N/A	Accuracy:79.50 AUC:90.10	35
Total	**30**	**260247**	**25249**	**73489**	**3288**	**Average** **Accuracy: 90.69** **Sensitivity:91.48** **Specificity:92.26** **AUC: 94.46**	

A summary of the results obtained by models using X-Ray images is illustrated in Table 11. Papers with their Accuracy, AUC, Sensitivity and Specificity are given along with their distribution of COVID-19 images in testing training and validation set like Table 10. It can also be seen that CT image-based models gained a minimum accuracy of 89.82% for the paper [14] and maximum accuracy of 99.94% for the paper [26]. For both Table 10 and Table 11 the publication date, the total number of images used by the respective papers is provided. Also, cited by (Number of papers) indicates the total number of papers that have cited the specific paper up to July 10, 2020.

Table 11: Summary of result evaluation for X-Ray images

COVID-19							
Publication Date	**Publication**	**Total Image**	**Training**	**Testing**	**Validation**	**Result (%)**	**Cited By(No of papers)**
March 24, 2020	[8]	50	10	5	10	Accuracy: 90.00 Sensitivity:100.00 Precision:100.00 F1 Score: 91.0 AUC:90.00	38
March 24, 2020	[9]	100	40	10	8	Accuracy:98.00 Sensitivity:96.00 Specificity:100.00 Precision:100.00 F1 Score:98.00	93
March 25, 2020	[10]	1427	202	22	N/A	Accuracy:96.78 Sensitivity:98.66 Specificity:96.46	86
March 27, 2020	[13]	1531	70	30	N/A	Accuracy:96.00 AUC:95.18	35
March 27, 2020	[14]	5941	54	14	N/A	Accuracy:89.82	19
March 29, 2020	[15]	3487	304	85	34	Accuracy:99.94	25
March 30, 2020	[17]	40	N/A	N/A	N/A	Accuracy:97.48 Sensitivity: 95.27 Specificity:99.70	5
March 31, 2020	[18]	170	120	50	N/A	Accuracy:98.00 Sensitivity:100.00 Specificity:96.00	11
March 31, 2020	[19]	13975	N/A	N/A	N/A	Accuracy:96.23 Precision:100.00 F1 Score:100.00	25
April 01, 2020	[20]	3905	409	46	N/A	Accuracy:99.18 Sensitivity:97.36 Specificity:99.42	9
April 02, 2020	[21]	5863	N/A	N/A	N/A	Accuracy:99.00 Precision:98.97 Sensitivity:98.97 F1 Score:98.97	9
April 09, 2020	[24]	16995	181	78	N/A	Accuracy:91.60 Sensitivity:92.45 Specificity:96.12	6
April 09, 2020	[25]	414	146	31	30	Accuracy:98.00	1
April 10, 2020	[26]	5216	Not specified	Not specified	Not specified	Accuracy:94.52	2
April 13, 2020	[30]	455	102	33	36	Accuracy:91.24 AUC:94.00	12
April 13, 2020	[31]	537	125	36	18	Accuracy:93.5 AUC:94.00	6
April 14, 2020	[33]	1300	N/A	N/A	N/A	Accuracy:89.60 Precision:93.00 Sensitivity:98.20	8
April 16, 2020	[35]	16700	286	27	N/A	Accuracy:99.01 AUC:99.72	4
April 16, 2020	[36]	864	70	50	N/A	Accuracy:95.70 Sensitivity:90.00 Specificity:95.80 AUC:97.00	19
April 17,2020	[40]	15085	149	31	N/A	Accuracy:99.56 Sensitivity:80.53	3
April 20,2020	[41]	5071	31	40	N/A	Sensitivity:97.50 Specificity:95.00 AUC:99.60	8
April 22,2020	[45]	381	Not	Not	Not	Accuracy:95.33	43

			specified	specified	specified	Sensitivity:95.33 F1 Score:95.34	
April 22,2020	[46]	274	137	Not specified	N/A	Accuracy:99.00	3
April 24,2020	[50]	109203	180	45	N/A	Accuracy:95.30	1
April 28,2020	[51]	13800	152	31	N/A	Accuracy:93.90	5
April 30,2020	[52]	59937	89	35	43	AUC:88.04	2
April 30,2020	[53]	11663	258	60	N/A	Precision:98.15 Sensitivity:88.33 AUC:98.50 F1 Score:92.98	1
April 30,2020	[54]	15111	175	20	20	Accuracy:89.40	0
May 01,2020	[55]	6297	105	10	10	Accuracy:97.10	1
May 05,2020	[56]	502	126	36	18	Accuracy:88.90 Specificity:96.40 F1 Score:84.40	9
May 06,2020	[57]	1144	63	27	N/A	F1 Score: 89.60	8
May 08,2020	[59]	6286	370	92	Stratified 5-fold cross-validation	Accuracy:95.90 Sensitivity:98.50 Specificity:95.70	3
May 11,2020	[60]	13975	258	100	N/A	Accuracy:93.30 Sensitivity:91.00 F1 Score:98.90	128
May 17,2020	[61]	196	74	31	N/A	Accuracy:95.12	18
May 21,2020	[63]	2239	191	48	N/A	Accuracy:97.01	4
May 23,2020	[64]	701	270	85	68	Accuracy:97.73	0
June 07,2020	[67]	5824	4659	1165	N/A	Accuracy:99.49 Sensitivity:99.43 Specificity:99.81	0
June 18,2020	[69]	30099	88	11	N/A	Accuracy:98.00 AUC:99.00	2
June 16,2020	[70]	15282	286	100	N/A	Accuracy:98.06	0
June 23,2020	[71]	51960	736	314	N/A	Accuracy:97.54 Sensitivity:97.88 Specificity:97.15	0
June 23,2020	[72]	2071	350	150	N/A	Accuracy:98.90	0
June 11, 2020	[73]	8474	7626	848	N/A	Accuracy:98.60	0
June 18, 2020	[74]	3300	247	62	N/A	Sensitivity:100.00 Specificitu:99.50	0
May June	[75]	50	20	5	N/A	Accuracy:91.00 Sensitivity:100.00 Specificity:80.00	0
June 19,2020	[76]	1312	228	65	33	Accuracy:97.40 Sensitivity:85.15 Specificity:99.05	0
June 09,2020	[77]	6523	N/A	N/A	N/A	Accuracy:98.00 Sensitivity:96.00 Specificity:98.00	0
June 20,2020	[78]	305	N/A	N/A	N/A	Accuracy:97.40	0
June 18,2020	[79]	35500	7340	7340	500	Accuracy:98.00	0
June 09,2020	[80]	1262	100	54	N/A	Sensitivity:90.74 Specificity:95.57	1
June 10,2020	[81]	1302	142	94	N/A	Precision:88.90 Sensitivity: 85.10	0
June 02,2020	[82]	754	302	75	5 fold cross validations	Accuracy:97.37	0
June 08,2020	[83]	1419	106	26	k fold cross validation	Accuracy:98.94 Sensitivity:96.00	0
Total	**52**	**506272**	**26977**	**11517**	**828**	**Average Accuracy:96.00 Sensitivity:91.09 Specificity:96.45 AUC:95.50**	

It can be said that the that X-Ray image-based models performed better than the CT image-based models by comparing Table 10 and Table 11.The average Accuracy, Sensitivity, Specificity and AUC for CT Image-based models are 90.69 %, 91.48%, 92.26%, and 94.46% and for X-Ray based models are 96.00%, 91.09%, 96.45%, and 95.50% respectively.

Conclusion:

As COVID-19 is spreading worldwide at a rapid rate, accurate and faster detection has become essential. In this article, we tried to present a comprehensive survey of AI-empowered methods that use medical images to combat the COVID-19 pandemic challenge by detecting it at a small cost and relatively faster in time. We surveyed 80 COVID-19 diagnosis models among which 28 were using CT images, 50 were using X-Ray images and 2 were using both CT and X-Ray images. Till now none of these models are proved to be as reliable to replace RT-PCR test and still researchers are trying to improve these techniques. From our survey, it is noticeable that the X-Ray image dataset is more widely available than the CT Image dataset as a CT scan is costly and more time-consuming. So most of the researchers utilized Chest X-ray images for diagnosing COVID-19. After analyzing several research work in this domain, we found out that there exists a shortage of annotated medical images of COVID-19 affected people. Enriching quality annotated medical images of COVID-19 affected people can play a significant role to boost up the performance of the mentioned data-hungry models. We remarked that using segmentation as preprocessing has a huge impact on model performance. We also observed that domain adoption in transfer learning is the widely used technique which gives promising result. Many researchers used Gradient-weighted Class Activation Mapping (Grad-CAM) with heatmap to interpret models output. Though this survey paper cannot claim to be an in-depth think about of those studies, but it presents a sensible outlook and shows a valid comparison of works in this field over these months which can be the conductor for the researcher to find future direction.

References

[1] Xiaowei Xu, Xiangao Jiang, Chunlian Ma, Peng Du, Xukun Li, Shuangzhi Lv, Liang Yu, Yanfei Chen, Junwei Su, Guanjing Lang, Yongtao Li, Hong Zhao, Kaijin Xu, Lingxiang Ruan, Wei Wu. Deep learning system to screen coronavirus disease 2019 pneumonia. arXiv:2002.09334. 2020 Feb 21

[2] Song Y, Zheng S, Li L, Zhang X, Zhang X, Huang Z, Chen J, Zhao H, Jie Y, Wang R, Chong Y. Deep learning enables accurate diagnosis of novel coronavirus (COVID-19) with CT images. medRxiv. 2020 Jan 1.

[3] Chen J, Wu L, Zhang J, Zhang L, Gong D, Zhao Y, Hu S, Wang Y, Hu X, Zheng B, Zhang K. Deep learning-based model for detecting 2019 novel coronavirus pneumonia on high-resolution computed tomography: a prospective study. MedRxiv. 2020 Jan 1.

[4] Li L, Qin L, Xu Z, Yin Y, Wang X, Kong B, Bai J, Lu Y, Fang Z, Song Q, Cao K. Artificial intelligence distinguishes COVID-19 from community acquired pneumonia on chest CT. Radiology. 2020 Mar 19:200905.

[5] Shi F, Xia L, Shan F, Wu D, Wei Y, Yuan H, Jiang H, Gao Y, Sui H, Shen D. Large-scale screening of covid-19 from community acquired pneumonia using infection size-aware classification. arXiv preprint arXiv:2003.09860. 2020 Mar 22.

[6] Jin S, Wang B, Xu H, Luo C, Wei L, Zhao W, Hou X, Ma W, Xu Z, Zheng Z, Sun W. AI-assisted CT imaging analysis for COVID-19 screening: Building and deploying a medical AI system in four weeks. medRxiv. 2020 Jan 1.

[7] Gozes O, Frid-Adar M, Greenspan H, Browning PD, Zhang H, Ji W, Bernheim A, Siegel E. Rapid ai development cycle for the coronavirus (covid-19) pandemic: Initial results for automated detection & patient monitoring using deep learning ct image analysis. arXiv preprint arXiv:2003.05037. 2020 Mar 10.

[8] Hemdan EE, Shouman MA, Karar ME. Covidx-net: A framework of deep learning classifiers to diagnose covid-19 in x-ray images. arXiv preprint arXiv:2003.11055. 2020 Mar 24.

[9] Narin A, Kaya C, Pamuk Z. Automatic detection of coronavirus disease (covid-19) using x-ray images and deep convolutional neural networks. arXiv preprint arXiv:2003.10849. 2020 Mar 24.

[10] Apostolopoulos ID, Mpesiana TA. Covid-19: automatic detection from x-ray images utilizing transfer learning with convolutional neural networks. Physical and Engineering Sciences in Medicine. 2020 Apr 3:1.

[11] Wang S, Zha Y, Li W, Wu Q, Li X, Niu M, Wang M, Qiu X, Li H, Yu H, Gong W. A fully automatic deep learning system for COVID-19 diagnostic and prognostic analysis. European Respiratory Journal. 2020 Jan 1.

[12] Zheng C, Deng X, Fu Q, Zhou Q, Feng J, Ma H, Liu W, Wang X. Deep learning-based detection for COVID-19 from chest CT using weak label. medRxiv. 2020 Jan 1.

[13] Zhang J, Xie Y, Li Y, Shen C, Xia Y. Covid-19 screening on chest x-ray images using deep learning based anomaly detection. arXiv preprint arXiv:2003.12338. 2020 Mar 27.

[14] Ghoshal B, Tucker A. Estimating uncertainty and interpretability in deep learning for coronavirus (COVID-19) detection. arXiv preprint arXiv:2003.10769. 2020 Mar 22.

[15] Chowdhury ME, Rahman T, Khandakar A, Mazhar R, Kadir MA, Mahbub ZB, Islam KR, Khan MS, Iqbal A, Al-Emadi N, Reaz MB. Can AI help in screening viral and COVID-19 pneumonia?. arXiv preprint arXiv:2003.13145. 2020 Mar 29.

[16] Fu M, Yi SL, Zeng Y, Ye F, Li Y, Dong X, Ren YD, Luo L, Pan JS, Zhang Q. Deep Learning-Based Recognizing COVID-19 and other Common Infectious Diseases of the Lung by Chest CT Scan Images. medRxiv. 2020 Jan 1.

[17] Hassanien AE, Mahdy LN, Ezzat KA, Elmousalami HH, Ella HA. Automatic x-ray covid-19 lung image classification system based on multi-level thresholding and support vector machine. medRxiv. 2020 Jan 1.

[18] Maghdid HS, Asaad AT, Ghafoor KZ, Sadiq AS, Khan MK. Diagnosing COVID-19 pneumonia from X-ray and CT images using deep learning and transfer learning algorithms. arXiv preprint arXiv:2004.00038. 2020 Mar 31.

[19] Farooq M, Hafeez A. Covid-resnet: A deep learning framework for screening of covid19 from radiographs. arXiv preprint arXiv:2003.14395. 2020 Mar 31.

[20] Apostolopoulos ID, Aznaouridis SI, Tzani MA. Extracting possibly representative COVID-19 Biomarkers from X-Ray images with Deep Learning approach and image data related to Pulmonary Diseases. Journal of Medical and Biological Engineering. 2020 May 14:1.

[21] Khalifa NE, Taha MH, Hassanien AE, Elghamrawy S. Detection of coronavirus (COVID-19) associated pneumonia based on generative adversarial networks and a fine-tuned deep transfer learning model using chest X-ray dataset. arXiv preprint arXiv:2004.01184. 2020 Apr 2.

[22] Gozes O, Frid-Adar M, Sagie N, Zhang H, Ji W, Greenspan H. Coronavirus detection and analysis on chest ct with deep learning. arXiv preprint arXiv:2004.02640. 2020 Apr 6.

[23] Ozkaya U, Ozturk S, Barstugan M. Coronavirus (COVID-19) Classification using Deep Features Fusion and Ranking Technique. arXiv preprint arXiv:2004.03698. 2020 Apr 7.

[24] Karim M, Döhmen T, Rebholz-Schuhmann D, Decker S, Cochez M, Beyan O. Deepcovidexplainer: Explainable covid-19 predictions based on chest x-ray images. arXiv preprint arXiv:2004.04582. 2020 Apr 9.

[25] Ezzat D, Ella HA. GSA-DenseNet121-COVID-19: a hybrid deep learning architecture for the diagnosis of COVID-19 disease based on gravitational search optimization algorithm. arXiv preprint arXiv:2004.05084. 2020 Apr 9.

[26] Alom MZ, Rahman MM, Nasrin MS, Taha TM, Asari VK. COVID_MTNet: COVID-19 Detection with Multi-Task Deep Learning Approaches. arXiv preprint arXiv:2004.03747. 2020 Apr 7.

[27] He K, Zhang X, Ren S, Sun J. Deep residual learning for image recognition. InProceedings of the IEEE conference on computer vision and pattern recognition 2016 (pp. 770-778).

[28] Chen X, Yao L, Zhang Y. Residual Attention U-Net for Automated Multi-Class Segmentation of COVID-19 Chest CT Images. arXiv preprint arXiv:2004.05645. 2020 Apr 12.

[29] Ronneberger O, Fischer P, Brox T. U-net: Convolutional networks for biomedical image segmentation. InInternational Conference on Medical image computing and computer-assisted intervention 2015 Oct 5 (pp. 234-241). Springer, Cham.

[30] Hall LO, Paul R, Goldgof DB, Goldgof GM. Finding covid-19 from chest x-rays using deep learning on a small dataset. arXiv preprint arXiv:2004.02060. 2020 Apr 5.

[31] Li X, Li C, Zhu D. COVID-MobileXpert: On-Device COVID-19 Screening using Snapshots of Chest X-Ray. arXiv preprint arXiv:2004.03042. 2020.

[32] Hu S, Gao Y, Niu Z, Jiang Y, Li L, Xiao X, Wang M, Fang EF, Menpes-Smith W, Xia J, Ye H. Weakly supervised deep learning for covid-19 infection detection and classification from ct images. arXiv preprint arXiv:2004.06689. 2020 Apr 14.

[33] Khan AI, Shah JL, Bhat MM. Coronet: A deep neural network for detection and diagnosis of COVID-19 from chest x-ray images. Computer Methods and Programs in Biomedicine. 2020 Jun 5:105581.

[34] Wu YH, Gao SH, Mei J, Xu J, Fan DP, Zhao CW, Cheng MM. JCS: An explainable COVID-19 diagnosis system by joint classification and segmentation. arXiv preprint arXiv:2004.07054. 2020 Apr 15.

[35] Rajaraman S, Siegelman J, Alderson PO, Folio LS, Folio LR, Antani SK. Iteratively Pruned Deep Learning Ensembles for COVID-19 Detection in Chest X-rays. arXiv preprint arXiv:2004.08379. 2020 Apr 16.

[36] Afshar P, Heidarian S, Naderkhani F, Oikonomou A, Plataniotis KN, Mohammadi A. Covid-caps: A capsule network-based framework for identification of covid-19 cases from x-ray images. arXiv preprint arXiv:2004.02696. 2020 Apr 6.

[37] He X, Yang X, Zhang S, Zhao J, Zhang Y, Xing E, Xie P. Sample-Efficient Deep Learning for COVID-19 Diagnosis Based on CT Scans. medRxiv. 2020 Jan 1.

[38] Al-Karawi D, Al-Zaidi S, Polus N, Jassim S. Machine Learning Analysis of Chest CT Scan Images as a Complementary Digital Test of Coronavirus (COVID-19) Patients. medRxiv. 2020 Jan 1.

[39] Mobiny A, Cicalese PA, Zare S, Yuan P, Abavisani M, Wu CC, Ahuja J, de Groot PM, Van Nguyen H. Radiologist-Level COVID-19 Detection Using CT Scans with Detail-Oriented Capsule Networks. arXiv preprint arXiv:2004.07407. 2020 Apr 16.

[40] Rahimzadeh M, Attar A. A New Modified Deep Convolutional Neural Network for Detecting COVID-19 from X-ray Images. arXiv preprint arXiv:2004.08052. 2020 Apr 17.

[41] Minaee S, Kafieh R, Sonka M, Yazdani S, Soufi GJ. Deep-covid: Predicting covid-19 from chest x-ray images using deep transfer learning. arXiv preprint arXiv:2004.09363. 2020 Apr 20.

[42] Zhou T, Canu S, Ruan S. An automatic COVID-19 CT segmentation network using spatial and channel attention mechanism. arXiv preprint arXiv:2004.06673. 2020.

[43] Amyar A, Modzelewski R, Ruan S. Multi-task Deep Learning Based CT Imaging Analysis For COVID-19: Classification and Segmentation. medRxiv. 2020 Jan 1.

[44] Qiu Y, Liu Y, Xu J. MiniSeg: An Extremely Minimum Network for Efficient COVID-19 Segmentation. arXiv preprint arXiv:2004.09750. 2020 Apr 21.

[45] Sethy PK, Behera SK. Detection of coronavirus disease (covid-19) based on deep features. Preprints. 2020 Mar 19;2020030300:2020.

[46] Kassani SH, Kassasni PH, Wesolowski MJ, Schneider KA, Deters R. Automatic Detection of Coronavirus Disease (COVID-19) in X-ray and CT Images: A Machine Learning-Based Approach. arXiv preprint arXiv:2004.10641. 2020 Apr 22.

[47] Wang S, Kang B, Ma J, Zeng X, Xiao M, Guo J, Cai M, Yang J, Li Y, Meng X, Xu B. A deep learning algorithm using CT images to screen for Corona Virus Disease (COVID-19). MedRxiv. 2020 Jan 1.

[48] Polsinelli M, Cinque L, Placidi G. A Light CNN for detecting COVID-19 from CT scans of the chest. arXiv preprint arXiv:2004.12837. 2020 Apr 24.

[49] Huang G, Liu Z, Van Der Maaten L, Weinberger KQ. Densely connected convolutional networks. In Proceedings of the IEEE conference on computer vision and pattern recognition 2017 (pp. 4700-4708).

[50] Basu S, Mitra S. Deep Learning for Screening COVID-19 using Chest X-Ray Images. arXiv preprint arXiv:2004.10507. 2020 Apr 22.

[51] Luz EJ, Silva PL, Silva R, Silva L, Moreira G, Menotti D. Towards an Effective and Efficient Deep Learning Model for COVID-19 Patterns Detection in X-ray Images. CoRR. 2020.

[52] Yeh CF, Cheng HT, Wei A, Liu KC, Ko MC, Kuo PC, Chen RJ, Lee PC, Chuang JH, Chen CM, Chou NK. A Cascaded Learning Strategy for Robust COVID-19 Pneumonia Chest X-Ray Screening. arXiv preprint arXiv:2004.12786. 2020 Apr 24.

[53] Zhang Y, Niu S, Qiu Z, Wei Y, Zhao P, Yao J, Huang J, Wu Q, Tan M. COVID-DA: Deep Domain Adaptation from Typical Pneumonia to COVID-19. arXiv preprint arXiv:2005.01577. 2020 Apr 30.

[54] Goodwin BD, Jaskolski C, Zhong C, Asmani H. Intra-model Variability in COVID-19 Classification Using Chest X-ray Images. arXiv preprint arXiv:2005.02167. 2020 Apr 30.

[55] Lv D, Qi W, Li Y, Sun L, Wang Y. A cascade network for Detecting COVID-19 using chest x-rays. arXiv preprint arXiv:2005.01468. 2020 May 1.

[56] Oh Y, Park S, Ye JC. Deep learning covid-19 features on cxr using limited training data sets. IEEE Transactions on Medical Imaging. 2020 May 8.

[57] Pereira RM, Bertolini D, Teixeira LO, Silla Jr CN, Costa YM. COVID-19 identification in chest X-ray images on flat and hierarchical classification scenarios. Computer Methods and Programs in Biomedicine. 2020 May 8:105532.

[58] Sun L, Mo Z, Yan F, Xia L, Shan F, Ding Z, Shao W, Shi F, Yuan H, Jiang H, Wu D. Adaptive Feature Selection Guided Deep Forest for COVID-19 Classification with Chest CT. arXiv preprint arXiv:2005.03264. 2020 May 7.

[59] Yamac M, Ahishali M, Degerli A, Kiranyaz S, Chowdhury ME, Gabbouj M. Convolutional Sparse Support Estimator Based Covid-19 Recognition from X-ray Images. arXiv preprint arXiv:2005.04014. 2020 May 8.

[60] Wang L, Wong A. COVID-Net: A Tailored Deep Convolutional Neural Network Design for Detection of COVID-19 Cases from Chest X-Ray Images. arXiv preprint arXiv:2003.09871. 2020 Mar 22.

[61] Abbas A, Abdelsamea MM, Gaber MM. Classification of COVID-19 in chest X-ray images using DeTraC deep convolutional neural network. arXiv preprint arXiv:2003.13815. 2020 Mar 26.

[62] Fan DP, Zhou T, Ji GP, Zhou Y, Chen G, Fu H, Shen J, Shao L. Inf-Net: Automatic COVID-19 Lung Infection Segmentation from CT Images. IEEE Transactions on Medical Imaging. 2020 May 22.

[63] Li T, Han Z, Wei B, Zheng Y, Hong Y, Cong J. Robust Screening of COVID-19 from Chest X-ray via Discriminative Cost-Sensitive Learning. arXiv preprint arXiv:2004.12592. 2020 Apr 27.

[64] Tahir A, Qiblawey Y, Khandakar A, Rahman T, Khurshid U, Musharavati F, Kiranyaz S, Chowdhury ME. Coronavirus: Comparing COVID-19, SARS and MERS in the eyes of AI. arXiv preprint arXiv:2005.11524. 2020 May 23.

[65] Ahuja S, Panigrahi BK, Dey N, Rajinikanth V, Gandhi TK. Deep transfer learning-based automated detection of COVID-19 from lung CT scan slices.

[66] Jin C, Chen W, Cao Y, Xu Z, Zhang X, Deng L, Zheng C, Zhou J, Shi H, Feng J. Development and Evaluation of an AI System for COVID-19 Diagnosis. medRxiv. 2020 Jan 1.

[67] Ahishali M, Degerli A, Yamac M, Kiranyaz S, Chowdhury ME, Hameed K, Hamid T, Mazhar R, Gabbouj M. A Comparative Study on Early Detection of COVID-19 from Chest X-Ray Images. arXiv preprint arXiv:2006.05332. 2020 Jun 7.

[68] Zhao J, Zhang Y, He X, Xie P. COVID-CT-Dataset: a CT scan dataset about COVID-19. arXiv preprint arXiv:2003.13865. 2020 Mar 30.

[69] Punn NS, Agarwal S. Automated diagnosis of COVID-19 with limited posteroanterior chest X-ray images using fine-tuned deep neural networks. arXiv preprint arXiv:2004.11676. 2020 Apr 23.

[70] Liu B, Yan B, Zhou Y, Yang Y, Zhang Y. Experiments of Federated Learning for COVID-19 Chest X-ray Images.

[71] Abbas A, Abdelsamea M, Gaber M. 4S-DT: Self Supervised Super Sample Decomposition for Transfer learning with application to COVID-19 detection. medRxiv. 2020 Jan 1.

[72] Shelke A, Inamdar M, Shah V, Tiwari A, Hussain A, Chafekar T, Mehendale N. Chest X-ray classification using Deep learning for automated COVID-19 screening. medRxiv. 2020 Jan 1.

[73] Heidari M, Mirniaharikandehei S, Khuzani AZ, Danala G, Qiu Y, Zheng B. Improving performance of CNN to predict likelihood of COVID-19 using chest X-ray images with preprocessing algorithms. arXiv preprint arXiv:2006.12229. 2020 Jun 11.

[74] Boudrioua MS. COVID-19 detection from chest X-ray images using CNNs models: Further evidence from Deep Transfer Learning. Available at SSRN 3630150. 2020 Jun 18.

[75] Manapure P, Likhar K, Kosare H. Detecting COVID-19 in X-ray images with Keras, Tensor Flow, and Deep Learning.

[76] Al-antari MA, Hua CH, Lee S. Fast Deep Learning Computer-Aided Diagnosis against the Novel COVID-19 pandemic from Digital Chest X-ray Images.

[77] Brunese L, Mercaldo F, Reginelli A, Santone A. Explainable Deep Learning for Pulmonary Disease and Coronavirus COVID-19 Detection from X-rays. Computer Methods and Programs in Biomedicine. 2020 Jun 20:105608.

[78] Mahmud T, Rahman MA, Fattah SA. CovXNet: A multi-dilation convolutional neural network for automatic COVID-19 and other pneumonia detection from chest X-ray images with transferable multi-receptive feature optimization. Computers in Biology and Medicine. 2020 Jun 20:103869.

[79] Asif S, Wenhui Y, Jin H, Tao Y, Jinhai S. Classification of COVID-19 from Chest X-ray images using Deep Convolutional Neural Networks. medRxiv. 2020 Jan 1.

[80] Salih SQ, Abdulla HK, Ahmed ZS, Surameery NM, Rashid RD. Modified AlexNet Convolution Neural Network For Covid-19 Detection Using Chest X-ray Images. Kurdistan Journal of Applied Research. 2020 Jun 9:119-30.

[81] Chatterjee S, Saad F, Sarasaen C, Ghosh S, Khatun R, Radeva P, Rose G, Stober S, Speck O, Nürnberger A. Exploration of Interpretability Techniques for Deep COVID-19 Classification using Chest X-ray Images. arXiv preprint arXiv:2006.02570. 2020 Jun 3.

[82] Tabik S, Gómez-Ríos A, Martín-Rodríguez JL, Sevillano-García I, Rey-Area M, Charte D, Guirado E, Suárez JL, Luengo J, Valero-González MA, García-Villanova P. COVIDGR dataset and COVID-SDNet methodology for predicting COVID-19 based on Chest X-Ray images. arXiv preprint arXiv:2006.01409. 2020 Jun 2.

[83] Singh KK, Siddhartha M, Singh A. Diagnosis of Coronavirus Disease (COVID-19) from Chest X-Ray images using modified XceptionNet. ROMANIAN JOURNAL OF INFORMATION SCIENCE AND TECHNOLOGY. 2020 Jan 1;23:S91-105.

[84] de la Iglesia Vayá M, Saborit JM, Montell JA, Pertusa A, Bustos A, Cazorla M, Galant J, Barber X, Orozco-Beltrán D, García-García F, Caparrós M. BIMCV COVID-19+: a large annotated dataset of RX and CT images from COVID-19 patients. arXiv preprint arXiv:2006.01174. 2020 Jun.

[85] Simonyan K, Zisserman A. Very deep convolutional networks for large-scale image recognition. arXiv preprint arXiv:1409.1556. 2014 Sep 4.

[86] Szegedy C, Liu W, Jia Y, Sermanet P, Reed S, Anguelov D, Erhan D, Vanhoucke V, Rabinovich A. Going deeper with convolutions. InProceedings of the IEEE conference on computer vision and pattern recognition 2015 (pp. 1-9).

[87] Szegedy C, Vanhoucke V, Ioffe S, Shlens J, Wojna Z. Rethinking the inception architecture for computer vision. InProceedings of the IEEE conference on computer vision and pattern recognition 2016 (pp. 2818-2826).

[88] Szegedy C, Ioffe S, Vanhoucke V, Alemi AA. Inception-v4, inception-resnet and the impact of residual connections on learning. InThirty-first AAAI conference on artificial intelligence 2017 Feb 12.

[89] Deng J, Dong W, Socher R, Li LJ, Li K, Fei-Fei L. Imagenet: A large-scale hierarchical image database. In2009 IEEE conference on computer vision and pattern recognition 2009 Jun 20 (pp. 248-255). Ieee.

[90] Selvaraju RR, Cogswell M, Das A, Vedantam R, Parikh D, Batra D. Grad-cam: Visual explanations from deep networks via gradient-based localization. InProceedings of the IEEE international conference on computer vision 2017 (pp. 618-626).

[91] Shi F, Wang J, Shi J, Wu Z, Wang Q, Tang Z, He K, Shi Y, Shen D. Review of artificial intelligence techniques in imaging data acquisition, segmentation and diagnosis for covid-19. IEEE reviews in biomedical engineering. 2020 Apr 16.

[92] Ilyas M, Rehman H, Naït-Ali A. Detection of Covid-19 From Chest X-ray Images Using Artificial Intelligence: An Early Review. arXiv preprint arXiv:2004.05436. 2020 Apr 11.

[93] Ulhaq A, Khan A, Gomes D, Pau M. Computer Vision for COVID-19 Control: A Survey. arXiv preprint arXiv:2004.09420. 2020 Apr 15.

[94] Zhou B, Khosla A, Lapedriza A, Oliva A, Torralba A. Learning deep features for discriminative localization. InProceedings of the IEEE conference on computer vision and pattern recognition 2016 (pp. 2921-2929).

[95] Goodfellow I, Pouget-Abadie J, Mirza M, Xu B, Warde-Farley D, Ozair S, Courville A, Bengio Y. Generative adversarial nets. InAdvances in neural information processing systems 2014 (pp. 2672-2680).

[96] LeCun Y, Haffner P, Bottou L, Bengio Y. Object recognition with gradient-based learning. InShape, contour and grouping in computer vision 1999 (pp. 319-345). Springer, Berlin, Heidelberg.

[97] Cortes C, Vapnik V. Support-vector networks. Machine learning. 1995 Sep 1;20(3):273-97.

[98] Chen T, Guestrin C. Xgboost: A scalable tree boosting system. In Proceedings of the 22nd acm sigkdd international conference on knowledge discovery and data mining 2016 Aug 13 (pp. 785-794).

[99] Schapire RE. A brief introduction to boosting. InIjcai 1999 Jul 31 (Vol. 99, pp. 1401-1406).

[100] Breiman L. Bagging predictors. Machine learning. 1996 Aug 1;24(2):123-40.

[101] Ke G, Meng Q, Finley T, Wang T, Chen W, Ma W, Ye Q, Liu TY. Lightgbm: A highly efficient gradient boosting decision tree. InAdvances in neural information processing systems 2017 (pp. 3146-3154).

[102] Milletari F, Navab N, Ahmadi SA. V-net: Fully convolutional neural networks for volumetric medical image segmentation. In2016 fourth international conference on 3D vision (3DV) 2016 Oct 25 (pp. 565-571). IEEE.

[103] Vaswani A, Shazeer N, Parmar N, Uszkoreit J, Jones L, Gomez AN, Kaiser Ł, Polosukhin I. Attention is all you need. In Advances in neural information processing systems 2017 (pp. 5998-6008).

[104] Nair V, Hinton GE. Rectified linear units improve restricted boltzmann machines. InICML 2010 Jan 1.